Coupled GSI-SVAT Model with Groundwater-Surface Water Interaction in the Riparian Zone of Tarim River

Sulitan Danierhan, Ph.D.[1]; Shalamu Abudu[2]; and Guan Donghai[3]

Abstract: The Tarim River is located in the arid areas of northwestern China, where groundwater (GW) and surface water (SW) in different landscape units have undergone regular and duplicate transformation processes, greatly improving the utilization of water resources. Investigation of the interaction between groundwater and surface water is critical to determine proper water resources planning and management in the Tarim River region. A new approach of coupling the soil-vegetation-atmosphere transport model (SVAT) with the groundwater-surface water interaction model (GSI) is presented in this paper. Usually, the surface water recharges to groundwater and groundwater-soil water exchange are not considered in the SVAT model. However, in reality, the soil water content profiles and soil heat profiles are intensely affected by shallow groundwater table, especially in arid riparian zones where groundwater levels fluctuate substantially. A new method linking the SVAT model with the GSI model is proposed in this paper to approach this issue. The groundwater-soil water exchange and groundwater evaporation can be effectively simulated using GW-SW interface in the coupled GSI-SVAT model. The coupled model is validated in the riparian zone of the upper reaches of the Tarim River with the simulation of heat and water transfer between groundwater level and soil surface, evapotranspiration, root water uptake, and groundwater-soil water exchange. The simulation results show good consistency with experimental data, indicating that the use of this coupled model could improve the accuracy of simulation of ecological water consumption in the riparian zone. The coupled GSI-SVAT model could be used for better planning and management of water resources in arid areas. **DOI: 10.1061/(ASCE)HE.1943-5584.0000732.** *© 2013 American Society of Civil Engineers.*

CE Database subject headings: Coupling; Geographic information systems; Simulation; Surface water; Groundwater management; Riparian water; China.

Author keywords: Coupled; Groundwater-surface water interaction soil-vegetation-atmosphere transport (GSI-SVAT) model; Simulation; Groundwater-surface water interaction.

Introduction

Water shortages have become increasingly serious in northwestern China (Wang et al. 2009), especially in arid and semiarid regions. As one of the main factors that limit development in local economies, water scarcity also brings ecosystem stability in regions such as the Tarim plain. The ecological water use in the Tarim River Basin has been affected significantly by the increasing agricultural water use in the basin. The climate in the Tarim plain is arid and characterized by little precipitation and very high evapotranspiration. The annual average precipitation is approximately 50 mm, whereas the annual average evapotranspiration is roughly 2,600 mm.

Predicting and simulating ecological water consumption is imperative for enhancing and managing water resources in arid and semiarid regions (Mo et al. 2005; Yurekli and Kurunc 2006; Ezzahar et al. 2007; Sevigne et al. 2011; Luo and Sophocleous 2011). Natural vegetation is a key consumer of water, so simulating and predicting the amount of water consumed by natural vegetation is crucial to developing the ecohydrology and protecting the natural ecosystem in this area. Populus euphratica, tamarix, reed, liquorice, and apocynum venetum are the dominating desert shrubs in the Tarim River Basin, and they use more than 80% of the total available water (Song et al. 2000). Dating back to the 1950s, models have been used to analyze water consumption. The first model was abandoned because the results consisted of uncertain variables, which produced operational difficulties that were later overcome by Lofting and McGauhey (1968). Velázquez (2006) introduced an input-output model, which established a numeric indicator for water consumption. His model was later developed by Wang et al. (2009) and used to analyze the direct and total water consumption of Zhangye in northwestern China. Recent studies have predicted water consumption using a variety of approaches, such as multiple regression methods, mathematical models, time series models, and even a neural network model (Lahlou and Colyer 2000; Froukh 2001). Firat et al. (2010) proposed a neural network model to predict monthly water consumption. Edwards et al. (2008) developed an aggregate water consumption model linked with a water resource model based on a composite population of water consumers.

For this reason, soil-vegetation-atmosphere transfer models have been developed by a number of investigators to simulate the soil water and heat transfer without a groundwater table variable

[1]Associate Researcher, State Key Laboratory of Desert and Oasis Ecology, Xinjiang Institute of Ecology and Geography, Chinese Academy of Sciences, No. 818 South Beijing Rd., Urumqi 830011, China (corresponding author). E-mail: sulitan@ms.xjb.ac.cn

[2]Researcher, Xinjiang Institute of Water Resources and Hydroelectric Sciences, No. 73 North Hongyanchi Rd., Urumqi 830049, China. E-mail: shalamu@yahoo.cn

[3]Senior Engineer, Xinjiang Institute of Water Resources and Hydroelectric Sciences, No. 73 North Hongyanchi Rd., Urumqi 830049, China. E-mail: xjskygdh@163.com

Note. This manuscript was submitted on November 15, 2011; approved on October 23, 2012; published online on October 25, 2012. Discussion period open until March 1, 2014; separate discussions must be submitted for individual papers. This paper is part of the ***Journal of Hydrologic Engineering***, Vol. 18, No. 10, October 1, 2013. © ASCE, ISSN 1084-0699/2013/10-1211-1218/$25.00.

(Braud et al. 1995; Prunty 2002; Kuchment et al. 2006; Romano and Giudici 2007; Wu et al. 2007; Kunstmann 2008; Petropoulos et al. 2009). The soil-vegetation-atmosphere transport (SVAT) model comes with several different expressions, including SVAT, SPAC (soil-plant-atmosphere continuum), and SHAW (soil heat and water), all of which are used for the simulation of the water and heat transport process in the SPAC system and the transport of solutes and CO_2. However, there are limited literatures on the application of the models in the riparian zones. As a new attempt, this paper brings this model to the experiment in the riparian zone of the Tarim River in northwest China.

A new approach for coupling the soil-vegetation-atmosphere transport model with the groundwater-surface water interaction model (GSI) is suggested in this paper. The soil water content profiles and soil heat profiles are intensely affected by shallow groundwater table, especially in arid riparian zones where the groundwater table fluctuates substantially. However, the surface water recharges to the groundwater and groundwater-soil water interaction are not considered in the SVAT model. Hence, an accurate simulation of the coupled GSI-SVAT model would enhance the ability to understand interactions between atmosphere, vegetation, soil, and groundwater.

The major objectives of this research are to (1) simulate the heat and water transfer in soil-vegetation-atmosphere transport; and (2) increase the simulation accuracy of the SVAT model by the optimization of the parameters of the coupled GSI-SVAT model. The parameters of the soil-vegetation-atmosphere transfer system such as atmospheric conditions, vegetation characteristics, root water uptake rate, soil water and heat distributions, groundwater table, and daily distribution of evapotranspiration were analyzed in the riparian zone of the Tarim River upper reaches during the growing season.

Experimental Site

The experiment was conducted in Akesu Agricultural Ecosystem National Scientific Research Station, Chinese Academy of Sciences, in Akesu, Xinjiang, China. The site is located near the intersection of three Tarim River branches (Akesu River, Yeerqiang River, and Hotan River) (longitude 80°51′ E, latitude 40°37′ N) 1,028 m above sea level. Compared to regions with similar latitudes, the climate can be characterized by extremely high summer temperatures and evaporation rates (mean annual evaporation is 2,500 mm) and low winter temperatures and precipitation (mean annual precipitation is 45.7 mm). The annual mean temperature is 11.2°C with 207 days of the nonfrost season. There are 2,940 annual sunlight hours; the annual mean wind speed is 2.4 $m \cdot s^{-1}$, and annual mean solar radiation is 6,000 $MJ \cdot m^{-2}$. The climate in the site is arid, vulnerable to extreme fluctuations in water availability and annual air temperature. High mountains provide snowmelt runoff as the main water source.

Vegetation is sparse, consisting primarily of populous euphratica, tamarix, and reed. The populous euphratica, tamarix, and reed canopies at the site are approximately 500, 260, and 200 cm, respectively, covering approximately 30% of the area where the groundwater depth ranges from 1.5–2.6 m. A standard HOBO meteorological station is located at the center of the three plots, measuring hourly means of air temperature, relative humidity, vapor pressure, wind speed, and net radiation at a height of 3 m, and liquid precipitation in a funnel at the soil surface. In addition, soil temperature and water content were measured hourly at depths of 5, 10, 20, 40, 70, 110, and $110 + x$ cm intervals near the site using seven hydra probes (preinstalled in the soil profile), which were linked to a DT80 logger (Fig. 1). Groundwater depth level was measured daily using a self-recording water level gauge. The distance between the study area and the river channel was 150 m (Fig. 2).

Model Description

The proposed water consumption coupled model includes two interlinked submodels. First, a SVAT model simulates the vegetation characteristics, root water uptake, evaporation, transpiration, and soil water and heat transfer in the soil layers; second, a GSI model simulates the surface water recharge to the groundwater and the groundwater-soil water exchange.

SVAT Model

The soil-vegetation-atmosphere transport consists of a vertical, one-dimensional profile denoted by a layered system that extends from the atmosphere, vegetation canopy, and soil surface to a specified depth within the soil and the groundwater table (Fig. 1; Sulitan 2005). The SVAT model simulates combined heat and water fluxes within this vertical profile under two basic assumptions for the soil—the Richards' equation for water flow and Fourier's law for heat flow. Water and heat fluxes at the surface boundary include absorbed net radiation, long-wave radiation exchange, and the transfer of heat and vapor.

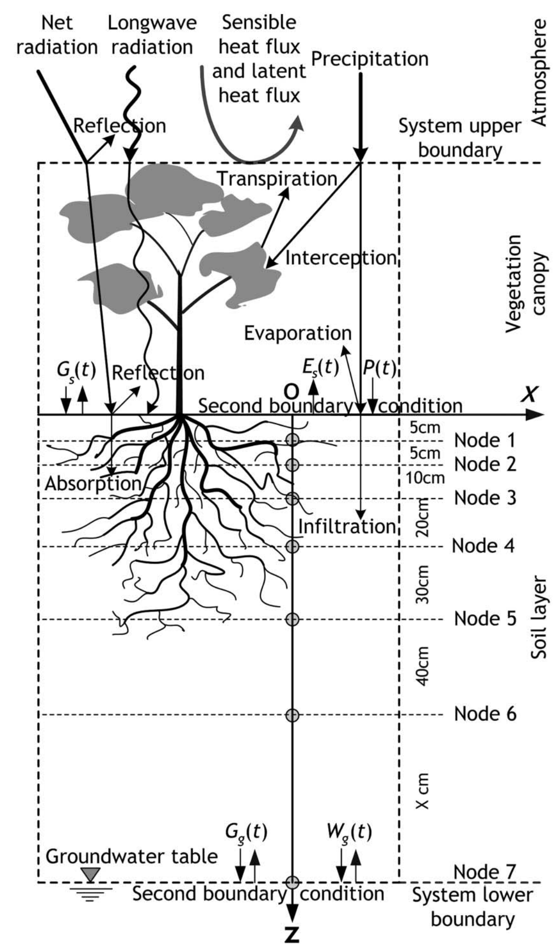

Fig. 1. Heat and water transfer in the soil-vegetation-atmosphere system

J. Hydrol. Eng. 2013.18:1211-1218.

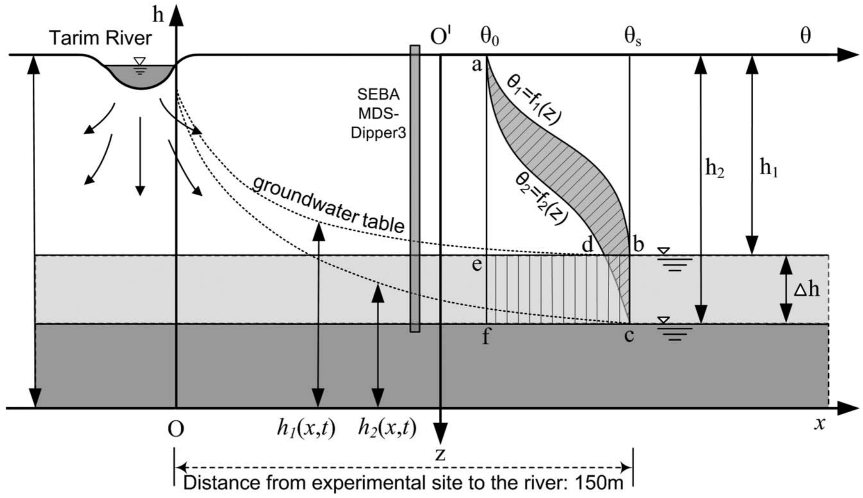

Fig. 2. Surface water-groundwater-soil water interaction in the riparian zone

Two linked submodels are a soil submodel that simulates water and heat fluxes in the unsaturated soil zone and a vegetation-atmosphere submodel that simulates vaporous water and heat fluxes in the vegetation canopy.

Soil Submodel in SVAT

Soil water content dynamics in the unsaturated zone are described by solving the diffusive form of Richards' equation (Sulitan 2005)

$$\frac{\partial \theta}{\partial t} = \frac{\partial}{\partial z}(D_{l\theta} + D_{s\theta})\frac{\partial \theta}{\partial z} + \frac{\partial}{\partial z}(D_{lT} + D_{sT})\frac{\partial T}{\partial z} + \frac{\partial K_{l\theta}}{\partial z} - S_w + P_w \tag{1}$$

where $T[k]$ = soil temperature; $\theta[\mathrm{m^3\,m^{-3}}]$ = volumetric soil water content; $z[\mathrm{m}]$ = soil depth; $K_{l\theta}[\mathrm{m\,s^{-1}}]$ = soil hydraulic conductivity; $D_{l\theta}[\mathrm{m^2\,s^{-1}}]$ = soil liquid water diffusivity of matric potential under isothermal condition; $D_{s\theta}[\mathrm{m^2\,s^{-1}}]$ = soil vaporous diffusivity of matric potential under isothermal condition; $D_{lT}[\mathrm{m^2\,K^{-1}\,s^{-1}}]$ = soil liquid water diffusivity of thermal potential; $D_{sT}[\mathrm{m^2\,K^{-1}\,s^{-1}}]$ = soil vaporous water diffusivity of thermal potential; $P_w[\mathrm{m^3\,m^{-3}\,s^{-1}}]$ = infiltration rate of precipitation; and $S_w[\mathrm{m^3\,m^{-3}\,s^{-1}}]$ = root water uptake rate.

Soil thermodynamics in the unsaturated zone are described by solving the Fourier's law (Sulitan 2005)

$$C_h\frac{\partial T}{\partial t} = \frac{\partial}{\partial z}\left[\lambda\rho_w D_{s\theta}\frac{\partial \theta}{\partial z} + (K_h + \lambda\rho_w D_{sT})\frac{\partial T}{\partial z}\right] \tag{2}$$

where $\lambda[\mathrm{J\,kg^{-1}}]$ = latent heat of evaporation (Table 1); $\rho_w[\mathrm{kg\,m^{-3}}]$ = density of water (Table 1); $C_h[\mathrm{J\,m^{-3}\,K^{-1}}]$ = heat capacity; and $K_h[\mathrm{J\,m^{-1}\,K^{-1}\,s^{-1}}]$ = thermal conductivity of soil.

$$D_{l\theta} = K_{L\theta}\frac{\partial \psi}{\partial \theta} \tag{3}$$

Table 1. Soil and Vegetation Related Parameters

Parameter	Result
ρ_w	1,000
λ	2,500,000
R_g	461.7
ξ	0.542
D	2.5816

where $\psi[\mathrm{m}]$ = matric potential depending nonlinearly on the soil water content θ and fractal dimension D (Table 1), which is given by

$$\psi = \psi_a((\theta/\theta_s)^{0.61} - 1)^{0.39} \tag{4}$$

The soil vaporous diffusivity of matric potential under isothermal condition is calculated as

$$D_{s\theta} = gTD_{sT}/\lambda \tag{5}$$

where the soil vaporous water diffusivity of thermal potential is given by

$$D_{sT} = \frac{\lambda\xi a D_a e_s(T)}{\rho_w T(R_v T)^2}\exp\left(\frac{g\psi}{R_g T}\right) \tag{6}$$

where $D_a = 0.96T^{1.88}[\mathrm{m^2\,s^{-1}}]$ = vapor diffusion coefficient; ξ = irregular coefficient of soil pore (Table 1); a = gas-phase volume ratio in the soil, $a = (\theta_s - \theta)$; $R_g[\mathrm{J\,kg^{-1}\,k^{-1}}]$ = water gas coefficient (Table 1); and $e_s(T)[Pa]$ = saturated vapor pressure, given by

$$e_s(T) = 6.1078\exp\left(17.269\frac{T - 273.16}{T - 35.19}\right) \tag{7}$$

The soil liquid water diffusivity of thermal potential D_{lT}, the thermal conductivity of soil K_h, and the heat capacity of soil C_h depend on the soil water content, which is given by

$$D_{lT} = -0.0068K_{l\theta}\psi\exp[-0.0237(293.16 - T)] \tag{8}$$

$$K_h = b_1 + b_2\theta + b_3\theta^{0.5} \tag{9}$$

$$C_h = 1.92(1 - \theta_s) + 4.18\theta \tag{10}$$

The soil hydraulic conductivity $K_{l\theta}$ is calculated as

$$K_{l\theta} = K_s\{1 - [(\theta/\theta_s)^{0.61} - 1]^{0.61}\}(\theta/\theta_s)^2(\theta/\theta_s)^{0.5} \tag{11}$$

where $\theta_s[\mathrm{m^3\,m^{-3}}]$ = volumetric soil water content; $K_s[\mathrm{m\,s^{-1}}]$ = soil hydraulic conductivity; and b_1, b_2, b_3 = thermal conductivity coefficients (Table 2).

The mechanisms of vegetation root water uptake play an important role in the water cycle of the soil-plant-atmosphere continuum. Water uptake at various depths below the ground surface

J. Hydrol. Eng. 2013.18:1211-1218.

Table 2. Soil and Groundwater Parameters

Parameter	Clay	Loam	Sand
K_s (m s^{-1})	0.2×10^{-5}	0.33×10^{-5}	2.5×10^{-5}
θ_s	0.52	0.48	0.44
A	0.7	1.9	3.4
m	0.3	0.4	0.5
a_1	0.119	0.132	0.149
a_2	2.471	2.733	3.125
a_3	0.257	0.281	0.293
b_1	−0.197	0.242	0.228
b_2	−0.962	0.393	−0.406
b_3	2.252	1.534	4.906

is primarily governed by root density, root depth, and the availability of water. The root water uptake rate accumulated from the soil within the root zone is approximately equal to the vegetation's total potential transpiration rate.

The total potential transpiration rate is obtained by integrating the accumulated root water absorption rate $S_w(z,t)$ over the whole root depth, which is formulated as follows:

$$T_v(t) = \int_{-lr}^{0} S_w(z,t)dz \tag{12}$$

$$S_w(z,t) = \frac{a_1}{l_r(t)} T_v(t) \cdot \exp\left\{-a_2\left[\frac{z}{l_r(t)} - a_3\right]^2\right\} \tag{13}$$

where $T_v(t)[\mathrm{m\,s^{-1}}]$ = transpiration rate of vegetation at time t; $S_w(z,t)[\mathrm{s^{-1}}]$ = transpiration rate of vegetation at time t; $l_r(t)[\mathrm{m}]$ = root depth into soil at time t along z coordinates; and a_1, a_2, and a_3 = fitting coefficients, in this study based on the relationship between root density $[\mathrm{g\,cm^{-3}}]$ and soil depth [m] by employing the least square method (Table 2).

Vegetation-Atmosphere Submodel in SVAT

Soil heat and water flow in the vegetation canopy are described by the energy balance equation

$$R_n = R_v + R_s \tag{14}$$

where $R_n[\mathrm{J\,m^{-2}\,s^{-1}}]$ = net radiation above the vegetation canopy; and R_v and R_s = net radiation in the vegetation canopy and soil surface, which is obtained by

$$R_v = VC.R_n\left[1 - \exp\left(-1.0 - 1.0364\left|\sin\frac{t-13}{12}\pi\right|\right)\mathrm{LAI}\right] \tag{15}$$

$$R_s = H_s + \lambda E_s + G \tag{16}$$

where VC = vegetation coverage; LAI = leaf area index; $G[\mathrm{J\,m^{-2}\,s^{-1}}]$ = ground heat flux; $H_s[\mathrm{J\,m^{-2}\,s^{-1}}]$ = sensible heat flux; and $\lambda E_s[\mathrm{J\,m^{-2}\,s^{-1}}]$ = latent heat flux that is calculated by

$$H_s = \rho_a C_p\Big[VC(T_s - T_c)/r_{sc} + (1-VC)\Big(T_s - T_{\mathrm{amin}} - T_{ar}\cos\frac{t-14}{12}\pi/r_{sa}\Big)\Big] \tag{17}$$

$$\lambda E_s = \frac{\rho_a C_p}{\gamma}\Big[VC\frac{e_s - e_c}{r_{sc}+r_s} + (1-VC)\Big(e_s - e_{\mathrm{amin}} - e_{ar}\cos\frac{t-14}{12}\pi\Big)/(r_{sa}+r_s)\Big] \tag{18}$$

where T_a[K] = atmosphere temperature; T_s[K] = soil surface temperature; T_c[K] = canopy temperature; T_{amin}[K] = days minimum air temperature; T_{ar}[K] = air temperature difference between maximum and minimum; $e_{\mathrm{amin}}[Pa]$ = days minimum air vapor pressure; $e_{ar}[Pa]$ = air vapor pressure difference between maximum and minimum; $e_s[Pa]$, $e_c[Pa]$, $e_{sc}[Pa]$ = soil vapor pressure, canopy vapor pressure, and vapor pressure of canopy to soil, respectively; and $r_s[\mathrm{s\,m^{-1}}]$, $r_{sc}[\mathrm{s\,m^{-1}}]$, and $r_{sa}[\mathrm{s\,m^{-1}}]$ = soil resistance, resistance of soil to canopy, and resistance of soil to atmosphere, respectively.

GSI Model

An important process in ecohydrology is groundwater-surface water interaction at the interface of riverbeds. Because of extreme water shortage, surface water supply from the Tarim River is not continuous in the study area. Hence, the groundwater recharge from the surface water is intermittent, which causes substantial groundwater table fluctuations during the irrigation season. The derivation process (the assumptions, physical setup, and derivation process) of the conversion of surface water and groundwater in the GSI submodel can be referred to Sulitan et al. (2003). The groundwater table variation is calculated by the interaction model between groundwater and surface water

$$\Delta h = S(x,t) = \begin{cases} \sum_{j=1}^{K}\frac{0.864A(Q_j^{1-m}-Q_{j-1}^{1-m})}{\sqrt{\pi}k\bar{h}}\left\{1-\frac{\sqrt{\pi}x}{2\sqrt{a(t_j-t_{j-1})}}+\sum_{n=0}^{\infty}\frac{(-1)^n x^{2(n+1)}}{[4a(t_j-t_{j-1})]^{n+1}(2n+1)(n+1)!}\right\}, & t \le t_0 \\ \sum_{j=1}^{K}(H_j - H_{j-1})\left\{1-\frac{1}{\pi}\times\sum_{n=0}^{\infty}\frac{(-1)^n x^{2n+1}}{\sqrt{a(t_j-t_{j-1})}[4a(t_j-t_{j-1})]^n(2n+1)n!}\right\}, & t > t_0 \end{cases} \tag{19}$$

where $t_0 = (\pi k^2\bar{h}^2h_0^2)/(0.746aA^2Q^{2-2\,m})$, Δh[m] = groundwater table variation; $Q[\mathrm{m^3\,s^{-1}}]$ = surface water flow; x[m] = direct distance from experimental point to the river; a = pressure conductivity of aquifer; H[m] = average water depth in the river; $\bar{h}$[m] = average thickness of aquifer; h_0[m] = initial water depth at time t_0; k = coefficient of permeability; and A, m = corrected coefficients relevant for soil water permeability, respectively (Table 2).

It has been recognized that groundwater and soil water interact closely with one another, especially in arid riparian zones where the groundwater levels fluctuate substantially. The groundwater-soil water exchanges through an interface are given by

J. Hydrol. Eng. 2013.18:1211-1218.

$$\Delta W = adcfa - abea = \int_0^{h_2} \theta_2(z)dz - \int_0^{h_1} \theta_1(z)dz \quad (20)$$

$$\Delta ET = cbef - \Delta W = \Delta h(\theta_s - \theta_0) - \int_0^{h_2} \theta_2(z)dz + \int_0^{h_1} \theta_1(z)dz \quad (21)$$

where $\Delta W[\mathrm{m\,s^{-1}}]$ = soil water variation; $ET[\mathrm{m\,s^{-1}}]$ = total evapotranspiration ($ET = E_s + T_v$); Δh is calculated by Eq. (19); θ_0 = initial soil water content; θ_s = saturated soil water content; h_1 = groundwater depth at time t_1; h_2 = groundwater depth at time t_2; and $\theta_2(z)$ and $\theta_1(z)$ = function of soil water content obtained by $\theta \sim z$ curve function from observed data in the unsaturated zone profile at time t_1 and t_2, respectively (Fig. 2).

Results and Discussions

The model was calibrated by using the sensitivity analysis method. The application of the GSI-SVAT model usually results in certain unstable parameters because of the complexity of system. Therefore, it is vital to analyze the sensitivity of those parameters to improve the precision and stability of the model. The sensitivity analysis method is as follows: to run the model, the values of certain parameters were adjusted in the range of 20–50% while maintaining the values of the other parameters unchanged; if a parameter was tested to be sensitive, it would be modified before inputting it into the model. Soil moisture content, soil temperature, vegetation transpiration, and ground surface evaporation were used as the targets in the sensitivity analysis. The analysis on meteorological parameters (air temperature, humidity, vapor pressure, wind speed, precipitation, net radiation, and vegetation coverage) and soil parameters (soil hydraulic conductivity and soil thermal conductivity) were conducted.

Simulation was run from June 28, 2010, to July 10, 2010, and model validation was accomplished by using data from the experimental sites in the riparian region in the summer of 2010. The observed and simulated hourly heat fluxes, such as latent heat flux, sensible heat flux, and ground heat flux in the vegetation canopy and near the surface ground are given in Fig. 3. Fig. 3 shows that the simulated heat flux reasonably trends to the observed heat flux and net radiation for the observational period.

Comparisons between observed and simulated values of water and heat fluxes show that simulated values of the latent heat flux, ground heat flux, soil temperature, and soil moisture are close to the observed values. As can be seen from Fig. 3, the simulated values by the GSI-SVAT model matched well with the observation values, indicating advantages of the coupling model compared to the single SVAT model. The coefficients of determination of observed and simulated hourly values of latent heat flux, sensible heat flux, and ground heat flux are 0.793, 0.684, and 0.833, respectively. Consequently, the relative errors of these simulated values and the observed values for the latent heat flux, sensible heat flux, and ground heat flux are 8.4, 13.4, and 5.2%, respectively.

Observed and simulated soil temperatures for the experimental sites are presented for the 5, 10, and 20 cm depths in Fig. 4. As can be seen from the figure, because the soil surface ground absorbs a

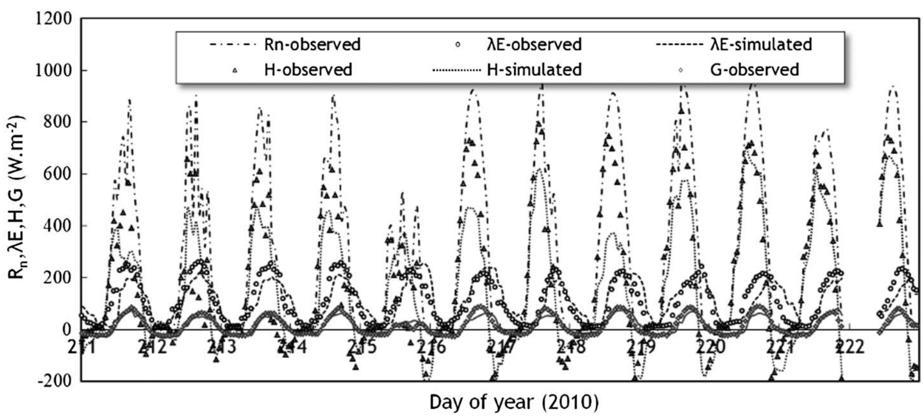

Fig. 3. Comparison between observed and simulated latent, sensible, and ground heat fluxes

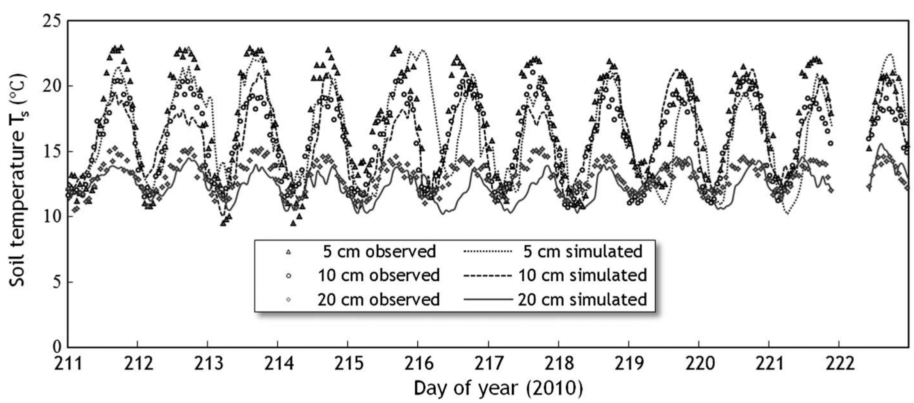

Fig. 4. Validation of GSI-SVAT model: observed and simulated average hourly soil temperature

J. Hydrol. Eng. 2013.18:1211-1218.

lot of net radiation compared to the deep soil depths, the soil temperature at the 5-cm depth fluctuates significantly. The coefficients of determination of observed and simulated hourly values of soil temperatures are 0.798, 0.883, and 0.661 for the 5, 10, and 20 cm depths, respectively. The relative errors between average hourly simulated values and the observed values for the 5, 10, and 20 cm depths are 11.2, 7.8, and 6.9%, respectively.

Fig. 5 presents the observed and simulated soil water contents for the 5, 10, and 20 cm depths. Because the soil profile near the ground surface follows the trends of temperature significantly, shallow soil profile holds much of the infiltrated and evapotranspirated water, resulting in a very high response at the 5-cm depth. Thus, the soil moisture at depths of 5 and 10 cm fluctuates greater than that at 20 cm.

The coefficients of determination of observed and simulated hourly values of soil water contents for the 5, 10, and 20 cm depths are 0.684, 0.399, and 0.373, respectively. The relative errors between the average hourly simulated values and the observed values for the 5, 10, and 20 cm depths are as small as 2.7, 1.8, and 1.6%, respectively. Consequently, the coupled model test

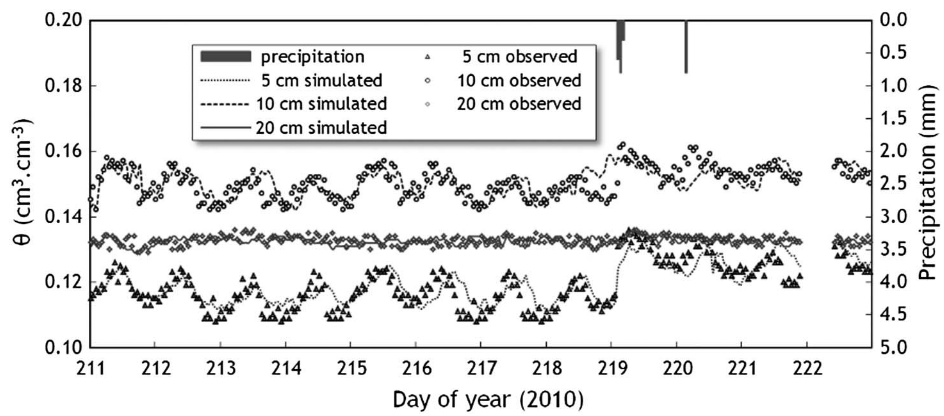

Fig. 5. Validation of GSI-SVAT model: observed and simulated average hourly soil water content

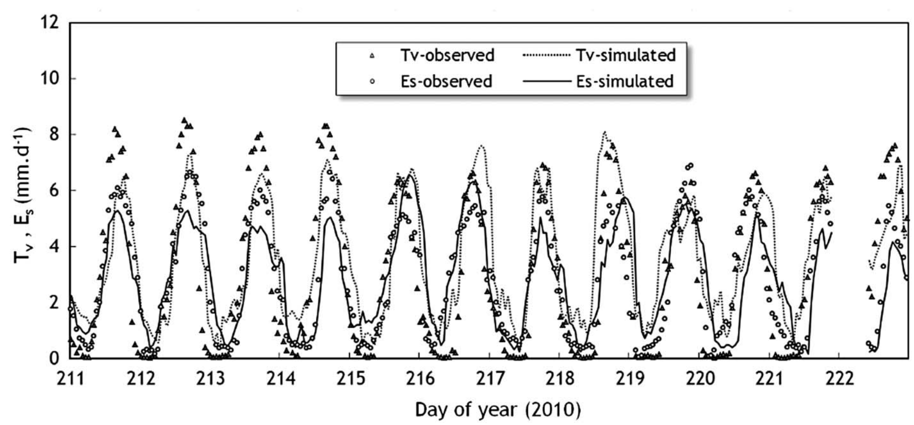

Fig. 6. Comparison of the simulated and observed values of evaporation and transpiration

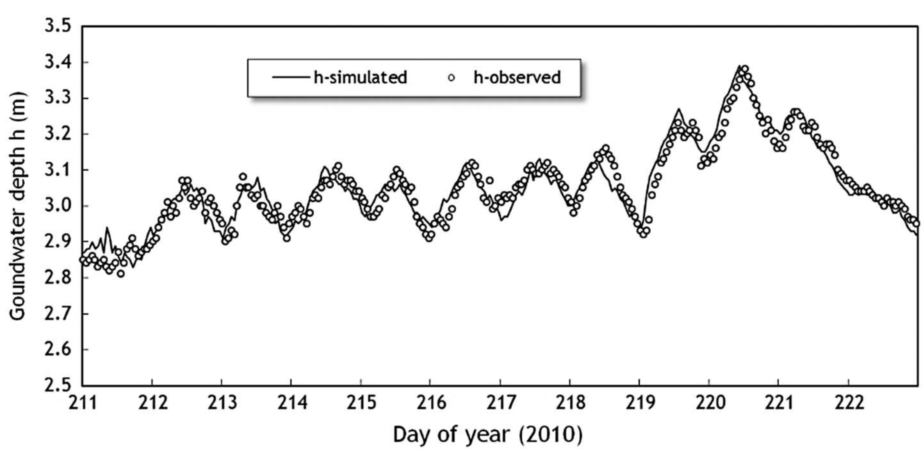

Fig. 7. Comparison of the simulated and observed values of groundwater depth

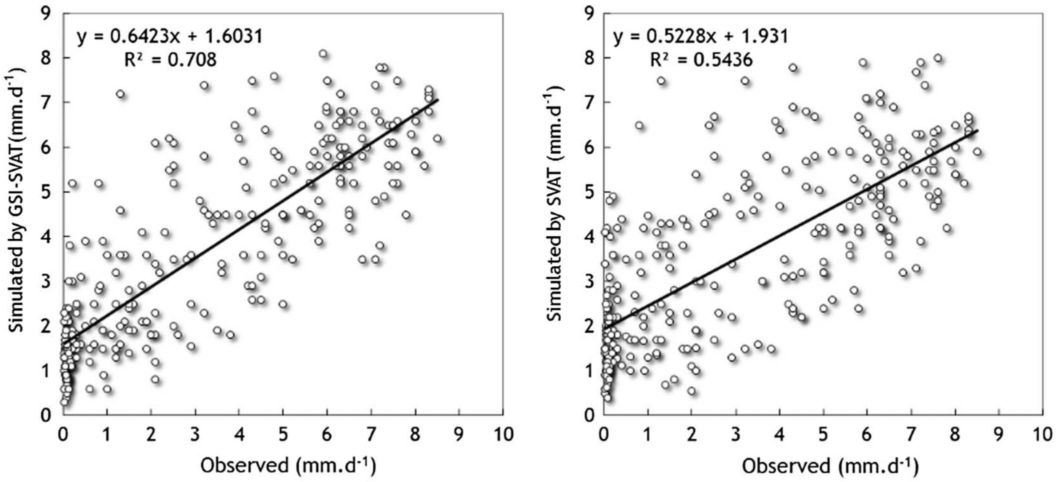

(a) (b)

Fig. 8. Comparison of simulation results by GSI-SVAT and SVAT (a) transpiration by GSI-SVAT model; (b) transpiration by SVAT model

against experimental data shows a good agreement between observed and simulated soil water contents at different soil profile depths.

Comparison of the simulated and observed values of the coupled GSI-SVAT model shows that the coefficients of determination of observed and simulated hourly values of transpiration and evaporation are 0.708 and 0.733, respectively. The relative errors of observed and simulated values for the evaporation and transpiration are 16.3 and 6.9%. (Fig. 6)

As can be seen from Fig. 7, the simulated groundwater depths closely fit the observed values by the GSI model. The coefficient of determination between observed and simulated groundwater depth is 0.898. The relative error of and simulated value with observed value for the groundwater depth is 1.2%.

Fig. 8 illustrates the SVAT model and GSI-SVAT model in their respective simulation of vegetation transpiration rate. As revealed, the simulated results by the GSI-SVAT model more approach the observed values. The coefficients of determination between simulated and observed transpiration are 0.708 and 0.544 by the GSI-SVAT model and SVAT model, respectively. The relative errors of simulated values of the SVAT model and GSI-SVAT model are respectively 6.9 and 9.2% against observed transpiration rates.

Conclusion

A coupled GSI-SVAT model that couples the soil-vegetation-atmosphere transport model with the groundwater-surface water interaction model was developed in this paper. This model describes the interaction between heat and water exchanges in the soil-vegetation-atmosphere system under two basic assumptions for the soil, i.e., the Richards' equation for water flow and Fourier's law for heat flow.

The coupled water GSI-SVAT model includes two interlinked submodels: first, a SVAT model simulates the vegetation characteristics, root water uptake, evaporation, transpiration, and soil water and heat transfer in the soil layers; second, a GSI model simulates the surface water recharge to the groundwater and the groundwater-soil water exchange.

The coupled model was validated in the riparian regions of the Tarim River upper reaches by simulating the heat and water transfer between the groundwater level and the soil surface, evapotranspiration, root water uptake, and groundwater-soil water exchanges. Comparisons between observed and simulated values of water and heat fluxes show that simulated values of the latent heat flux, ground heat flux, soil temperature, and soil moisture are close to the observed values.

The coupled GSI-SVAT model showed better performance compared to the single SVAT model in the arid lands. However, there are several limitations in the application of the coupled GSI-SVAT model to the entire watershed when using the scaling method. For example, the regional partition method is usually used in small areas, and its application to large-scale watersheds is difficult. In this case, the use of the coupled model shows a potential for linking other methods, such as remote sensing, and this may reduce the limitations of the GSI-SVAT model and improve its capabilities.

Acknowledgments

This research was supported by one of the National Natural Science Foundation of China (Grant No. 41071026, 51069017), Public Welfare Foundation of the Ministry of Water Resources of the People's Republic of China (Grant No. 201001065), and part of this work is commissioned by the National Basic Research Programs of China (2009CB421302).

References

Braud, I., Dantas-Antonino, A. C., Vauclin, M., Thony, J. L., and Ruelle, P. (1995). "A simple soil-plant-atmosphere transfer model (SiSPAT) development and field verification." *J. Hydrol.*, 166(3–4), 213–250.

Edwards, M., Goreaud, F., and Ferrand, N. (2008). "Simulating heterogeneity in a consumption model linked to a water resource model: When is the linear approximation relevant?" *Simul. Modell. Pract. Theory*, 16(1), 65–75.

Ezzahar, J., Chehbouni, A., Hoedjes, J. C. B., Er-Raki, S., Chehbouni, Ah., and Boulet, G. (2007). "The use of the scintillation technique for monitoring seasonal water consumption of olive orchards in a semi-arid region." *Agric. Water Manage.*, 89(3), 173–184.

Firat, M., Turan, M. E., and Yurdusev, M. A. (2010). "Comparative analysis of neural network techniques for predicting water consumption time series." *J. Hydrol.*, 384(1–2), 46–51.

Froukh, M. L. (2001). "Decision-support system for domestic water demand forecasting and management." *Water Resour. Res.*, 15(6), 362–382.

Kuchment, L. S., Demidov, V. N., and Startseva, Z. P. (2006). "Coupled modeling of the hydrological and carbon cycles in the soil-vegetation-atmosphere system." *J. Hydrol.*, 323(1–4), 4–21.

Kunstmann, H. (2008). "Effective SVAT-model parameters through inverse stochastic modeling and second-order first moment propagation." *J. Hydrol.*, 348(1–2), 13–26.

Lahlou, M., and Colyer, D. (2000). "Water conservation in Casablanca, Morocco." *J. Am. Water Resour. Assoc.*, 36(5), 1003–1012.

Lofting, E. M., and McGauhey, P. H. (1968). "Economic valuation of water. An input–output analysis of California water requirements." *Contribution*, 116, Univ. of California Water Resources Center, Berkeley, CA.

Luo, Y., and Sophocleous, M. (2011). "Two-way coupling of unsaturated-saturated flow by integrating the SWAT and MODFLOW models with application in an irrigation district in arid region of West China." *J. Arid Land*, 3(3), 164–173, 10.3724/SP.J.1227.2011.00164.

Mo, X., Liu, S., Lin, Z., Xu, Y., Xiang, Y., and McVicar, T. R. (2005). "Prediction of crop yield, water consumption and water use efficiency with a SVAT-crop growth model using remotely sensed data on the North China Plain." *Ecol. Model.*, 183(2–3), 301–322.

Petropoulos, G., Wooster, M. J., Carlson, T. N., Kennedy, M. C., and Scholze, M. (2009). "A global Bayesian sensitivity analysis of the 1d SimSphere soil-vegetation-atmospheric transfer (SVAT) model using Gaussian model emulation." *Ecol. Model.*, 220(19), 2427–2440.

Prunty, L. (2002). "Soil water heat of transport." *J. Hydrol. Eng.*, 7(6), 435–440.

Romano, E., and Giudici, W. (2007). "Experimental and modeling study of the soil-atmosphere interaction and unsaturated water flow to estimate the recharge of a phreatic aquifer." *J. Hydrol. Eng.*, 12(6), 573–584.

Sevigne, E., et al. (2011). "Water and energy consumption of Populus spp. bioenergy systems: A case study in Southern Europe." *Renew. Sust. Energ. Rev.*, 15(2), 1133–1140.

Song, Y. D., Fan, Z. L., Lei, Z. D., and Zhang, X. F. (2000). *Research on water resources and ecology of Tarim River in China*, Xinjiang People's Press, Urumqi, 457–478.

Sulitan, D. (2005). "Simulation of water and heat transfer at ecotone between oasis and desert." *Doctoral dissertation*, Hohai University, Nanjing, China, 21–48.

Sulitan, D., Song, Y. D., and Gulimire, H. (2003). "Reckoning of erfc (λ) and ierfc(λ) approximation formula in non-stable groundwater flows and their application in Tarim river watershed." *Arid Land Geog.*, 26(4), 323–328.

Velázquez, E. (2006). "An input–output model of water consumption: Analyzing intersectoral water relationships in Andalusia." *Ecol. Econ.*, 56(2), 226–240.

Wang, Y., Xiao, H. L., and Lu, M. F. (2009). "Analysis of water consumption using a regional input–output model: Model development and application to Zhangye City, Northwestern China." *J. Arid Environ.*, 73(10), 894–900.

Wu, C. L., Chao, K. W., and Huang, J. S. (2007). "Modelling coupled water and heat transport in a soil–mulch–plant–atmosphere continuum (SMPAC) system." *Appl. Math. Model.*, 31(2), 152–169.

Yurekli, K., and Kurunc, A. (2006). "Simulating agricultural drought periods based on daily rainfall and crop water consumption." *J. Arid Environ.*, 67(4), 629–640.

J. Hydrol. Eng. 2013.18:1211-1218.